

POSTBUCKLING MODE SHAPES OF COMPOSITE STIFFENED FUSELAGE PANELS INCORPORATING STOCHASTIC VARIABLES

M. Lee¹, D. Kelly¹, A.C. Orifici^{2,3} and R.S. Thomson³

¹School of Mechanical and Manufacturing Engineering, University of New South Wales
Sydney, NSW 2052
Australia

²School of Aerospace, Mechanical and Manufacturing Engineering, RMIT University
GPO Box 2476V, Melbourne, VIC 3001
Australia

³Cooperative Research Centre for Advanced Composite Structures Limited
506 Lorimer Street, Fishermans Bend, VIC 3207
Australia

OVERVIEW

The European Commission 6th Framework Project COCOMAT (Improved **MAT**erial Exploitation at Safe Design of **CO**mposite Airframe Structures by Accurate Simulation of **CO**llapse) is a four year project aimed at exploiting the large reserve of strength in composite structures through more accurate prediction of collapse. The Cooperative Research Centre for Advanced Composite Structures (CRC-ACS) Limited (Australia) is one of the 15 international partners involved in this project. During the initial benchmarking, it was found that the finite element solvers gave symmetric postbuckling mode shapes for the stiffened composite panels. These mode shapes did not reflect the experimental results obtained from the Deutsches Zentrum für Luft- und Raumfahrt (DLR), another COCOMAT partner, which gave asymmetrical mode shapes. The inability of the deterministic finite element models to capture the asymmetry has been noted to be the most significant factor affecting the numerical predictions for collapse and failure. A Stochastic Finite Element Analysis (SFEA) procedure involving the use of stochastic material, lamina and boundary conditions is proposed in this paper. Using stochastic variables in a finite element environment the asymmetrical postbuckling mode shapes have been captured, matching the modes seen in the experiments. It is expected that COCOMAT will produce a large amount of scatter in results due to the postbuckling modes. With the aid of the SFEA, it is also possible to redesign the experiment thereby reducing experimental scatter and therefore increasing the robustness of the system.

1. INTRODUCTION

Compared to traditional isotropic materials such as Aluminium, anisotropic composites are more complex to design and manufacture due to the multiple processes required in fabrication. Each step of the process includes scatter from geometrical and material properties that can affect the overall behaviour of the finished structure.

Buckling is a complex failure mode where the factors causing failure can sometimes be difficult to determine. With the use of finite element (FE) modelling, it is possible to investigate the causes of failure as the input variables in

the analysis are taken from nominal values. This is unlike the environment in which physical experiments are conducted where sources of variation from manufacture and loading can sometimes go undetected, thereby affecting the final result. Unfortunately in most cases where finite elements are used to model structures, only nominal design parameters are considered hence a perfect structure is always analysed. In reality such a state cannot possibly exist as input parameters are always stochastic in nature, occurring within a range determined by machine tolerance and other uncontrollable factors. Hence eccentricities will always exist in the loading of structures and in the case of composite laminates, no symmetrical lay-ups can possibly exist.

The currently running European Commission 6th Framework Project COCOMAT (Improved **MAT**erial Exploitation at Safe Design of **CO**mposite Airframe Structures by Accurate Simulation of **CO**llapse) is focused on exploiting the large postbuckling strength reserve in composite structures through more accurate prediction of collapse^[1]. The four year project is based around a comprehensive experimental test program involving material characterisation tests, small validation structures, and large, multi-stiffener panels representative of composite fuselage designs.

Curved panels such as those modelled numerically and tested physically in COCOMAT are suitable examples of how imperfection-sensitive stiffened composite panels can be. Both the physical experiments and numerical simulations exhibit different postbuckling mode shapes during compression^[2]. This difference in postbuckling mode shapes directly affects the loading capability of the stiffened panel, and the manner in which the stiffeners fail in global buckling.

With regards to accounting for variation in real structures, attempts have been made in the recent years to introduce imperfections via stochastic modelling so as to achieve plausible knock down factors. This can be seen in the work by Chryssanthopoulos and Poggi^[3]. Various FE codes such MSC.Nastran, MSC.Marc and Abaqus also currently allow for imperfection modelling to further draw in the reality of variation. Initial benchmark FE of COCOMAT panels by Orifici et al.^[4] has included this imperfection

feature in order to match load-shortening curves obtained through experimentation.

Raj et al.^[5] acknowledge that it is impossible to control all the variables in a manufacturing process, and hence for better understanding of structural behaviour, all material properties should be considered stochastic. It was found that thin plates with an aspect ratio less than 100 were found to be sensitive to deflection loading, and the longitudinal modulus and in-plane shear modulus were critical when plates were subjected to bending loads. Singh et al.^[6] note that although there is a wealth of understanding generated from deterministic analyses, structural analyses where the material properties are stochastic is still underdeveloped. Cylindrical panels were analysed and found to be sensitive to boundary conditions, aspect ratio as well as material properties, though the analyses did not investigate geometrical properties.

Yadav and Verma^[7] varied the aspect ratios of cylindrical composite panels and found that panels with low aspect ratios and high thickness ratios were more buckling sensitive. Noor et al.^[8] have concluded that cylindrical panels are most affected by edge displacement. A_{11} , the extensional component of the stiffness matrix was also identified as being a critical buckling parameter in a cylindrical panel. Their methodology involved the use of numerical sensitivity response techniques. The results do not contradict the results obtained by Singh et al.^[6] as a different methodology was used to conduct the stochastic experiments.

The introduction of uncertainty into composites has also been looked at by Shiao and Chamis^[9] with the aim of increasing reliability in the assembled structure. With the use of a software code IPACS (Integrated Probabilistic Assessment of Composite Structures) developed in-house at NASA, they were able to identify the sensitivity of input variables with respect to the output response in a probabilistic framework with the aim of conducting reliability assessments. This work was furthered by Chamis^[10] and it led towards the improvement of structural response with no increase in weight by means of tailoring the behaviour of the composite material.

Zimmermann et al.^[11] have done investigations in the axial buckling of stringer-stiffened fibre composite panels and found that the construction of the stiffeners affect the buckling capability of the composite panels. The manner in which the panels buckle, in the global mode, is determined by odd or even number of stiffeners employed.

Within the postbuckling region, it has also been found that boundary conditions will affect the achieved mode shape. Short et al.^[12] found that unstiffened panels were highly sensitive to the boundary conditions. Zimmermann et al.^[11] note that simple boundary conditions over-estimated the degree of restraint applied by clamps on the side edges of curved stiffened panels.

Employing stochastics to model advanced composite structures has not only been limited to curved cylinders and panels. In a recent paper by Marczyk^[13], a case was presented where a saddle appeared on composite reflector dishes manufactured by CASA-EADS Space Division. The deterministic finite element solutions had initially indicated that no saddling would occur in the dishes but this was proven false once variation was

introduced into the lamina orientations.

In a paper by Orifici et al.^[2] on the design and analysis of a COCOMAT postbuckling panel, it was stated that the asymmetrical postbuckling mode shapes achieved through physical testing were possibly due to three reasons, which include:

- 1) Warping of the panels at curing and manufacture
- 2) Imperfections in the stiffener blade width
- 3) Asymmetric introduction of the load on the panel

The benchmark finite element models did not include any of the imperfections above and hence no match with the benchmark experimental result was obtained. The experimental result followed by the FE results can be seen in FIG. 1 below, which compares the out of plane displacement patterns at specified axial displacement (in mm) of the experiment and various FE codes.

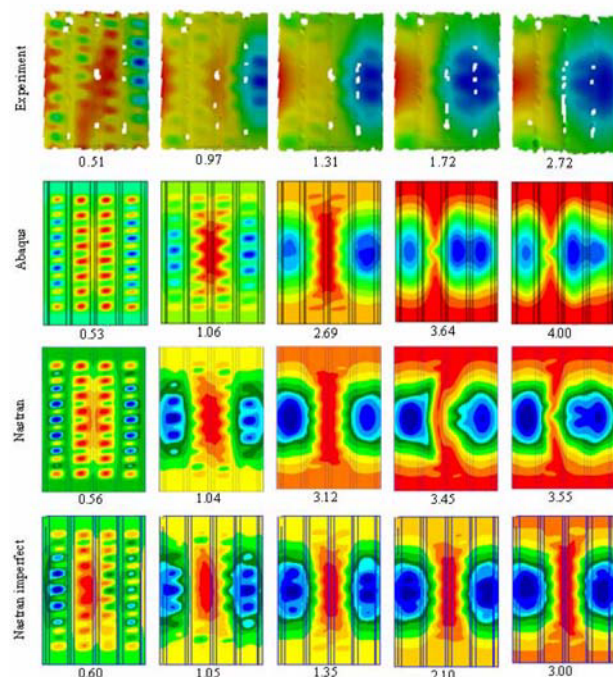


FIG. 1 Radial displacement at applied compression, benchmark results from experiment and FE^[2]

The inability of the deterministic approach to capture the panel asymmetric buckling pattern of the COCOMAT panels is similar to the saddling problem encountered by CASA-EADS where the predicted result differed from the actual result. In the same manner, the introduction of stochastic material and boundary conditions is expected to produce FE results having asymmetrical postbuckling mode shapes. The analysis of the curved panels is also further complicated through the role of the stiffeners. The addition of stiffeners and the application of the panels in the postbuckling region, means that the buckling deformation pattern, or mode, becomes a factor in the performance of the structure. The inclusion of stiffeners also affects the way in which the compression load is handled by the structure.

In this work, a stochastic analysis approach is applied to curved blade-stiffened panels from the COCOMAT project. The stochastic analysis methodology is first explained, and

two simple examples are given to illustrate its application. A stochastic finite element analysis (SFEA) is then performed on a fuselage-representative multi-stiffener COCOMAT panel. A key aspect of this analysis is a focus on the postbuckling mode shape as the dominant performance parameter. It is shown that the stochastic approach is able to achieve better and more realistic comparisons with experimental results than a deterministic analysis. Following this, recommendations are given for including the postbuckling mode shape as a design parameter, both in terms of experiment and panel design.

2. EXAMPLE OF STOCHASTIC METHODOLOGY

In a traditional multi-variable sensitivity analysis, the analysis is conducted by varying only one input variable and observing the change in response. This can be seen in the equation below.

$$(1) \quad \Delta Y = \left. \frac{\partial f}{\partial X_1} \right|_{\substack{x_2=a \\ x_n=b}}$$

The behaviour of the system in question can be quantified by determining the gradient. This may not reflect the true behaviour of the system under actual operating conditions, as it is not appropriate to consider input variables as being deterministic. Hence a new stochastic analysis procedure has been devised in order to account for this variability. With the introduction of variation into all the input variables, all the input variables should be considered stochastic in nature as follows:

$$(2) \quad \begin{aligned} X_1 &= f_1(\mu, \sigma) \\ X_n &= f_n(\mu, \sigma) \end{aligned}$$

where **X** is the random input variable
μ is the mean
σ is the standard deviation
n is the number of input variables

Hence the analysis can be described as multi-variant and each output result should consist of a combination of input variables as follows:

$$(3) \quad \begin{aligned} Y_1 &= f_1(X_1, X_2, X_z) \\ Y_m &= f_m(X_a, X_b, X_c) \end{aligned}$$

where **Y** is the output response
X is the input variable
m is the sample size

Therefore a stochastic analysis with **m** number sample size and **n** number input variables can be described as follows:

$$(4) \quad S_n^m = f_n(Y_1, Y_2, \dots, Y_m)$$

The variation of each sample point from the nominal design mean can be seen below:

$$(5) \quad \Delta Y_m = \left(\frac{\partial f}{\partial X_1} \right) \Delta X_1 + \left(\frac{\partial f}{\partial X_2} \right) \Delta X_2 + \dots + \left(\frac{\partial f}{\partial X_n} \right) \Delta X_n$$

From the stochastic analyses, **m** number of plots can be obtained, where the output response, **Y_m** is plot against the input variables, **X_{1,2,n}**. The figures below show the difference between a multi-variable and multi-variant analysis.

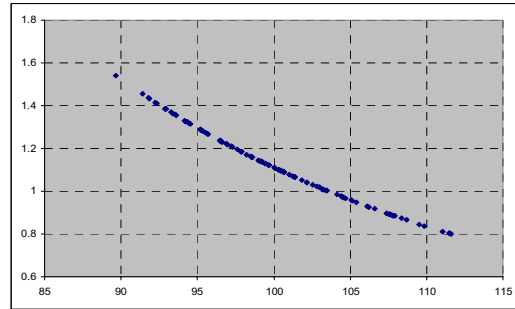


FIG. 2 Example of a multi-variable system

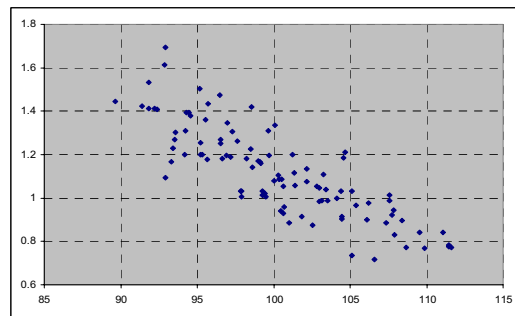


FIG. 3 Example of a multi-variant system

Once the response plots are generated, a Spearman Correlation^[14] is done in order to find the influence of input variable with respect to the output response. The Spearman Rank Correlation is a non-linear correlation which can be used at the ordinal level. Applying the Spearman Correlation, higher values correspond to a stronger relationship between variables. The formulation for the Spearman Correlation is:

$$(6) \quad \rho = \frac{\sum_{i=1}^n R(x_i)R(y_i) - n\left(\frac{n+1}{2}\right)^2}{\sqrt{\sum_{i=1}^n R(x_i)^2 - n\left(\frac{n+1}{2}\right)^2} \sqrt{\sum_{i=1}^n R(y_i)^2 - n\left(\frac{n+1}{2}\right)^2}}$$

where **R** is the ordinal rank
y is the output response
x is the input variable
n is the number of input variables

2.1 Example of Beam Deflection

An example of this methodology is demonstrated below. Consider a simple cantilevered beam with an edge loading as shown in FIG. 4 below.

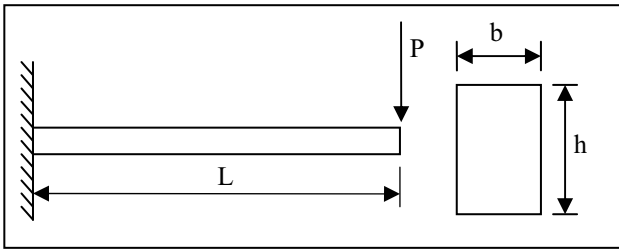


FIG. 4 Cantilevered beam with edge loading

The expected deflection, δ from the cantilevered beam is:

$$(7) \quad \delta = \frac{PL^3}{3EI}$$

The moment of inertia, I for the beam is:

$$(8) \quad I = \frac{bh^3}{12}$$

TAB. 1 below shows the stochastic boundary for this stochastic analysis. A standard deviation of 5% has been used for this example.

TABLE 1

Input Variable	Mean	Defined Range	
Load, P (N)	1 000	850	- 1 150
Length, L (mm)	1 000	850	- 1 150
Young's Modulus, E (MPa)	72 000	61 200	- 82 800
Breadth, b (mm)	50	42.5	- 57.5
Height, h (mm)	100	85	- 115

A sample size of 100 was used for the stochastic analysis. This allowed the following plots to be produced. Each plot, or metamodel, is the response with respect to the input variable. TAB. 2 shows the influence that the input variables have over the deflection of the beam. It can be seen that in this instance, the height of beam has the greatest influence over the deflection. This is due to the inverse cube effect of the height in the deflection equation.

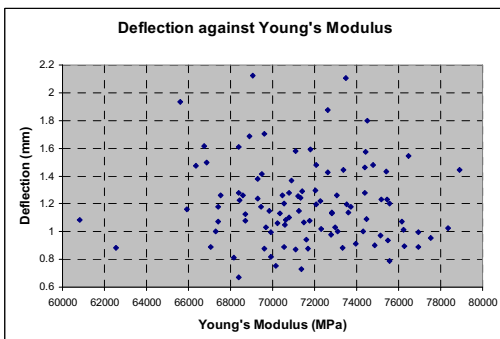


FIG. 5 Metamodel of deflection against Young's modulus

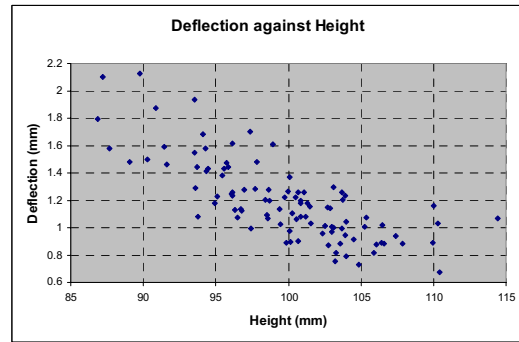


FIG. 6 Metamodel of deflection against height

TABLE 2

Relationship	Spearman Correlation
Displacement and Load	0.258
Displacement and Length	0.572
Displacement and Young's Modulus	-0.106
Displacement and Breadth	-0.266
Displacement and Height	-0.772

2.2 Example of Bifurcated System

The previous example showed the spread in the result once variation was taken into account. In this example, attempt is made to show the importance of stochastics in design. A two member system consisting of slender beams is subjected to an angular load is shown below in FIG. 7.

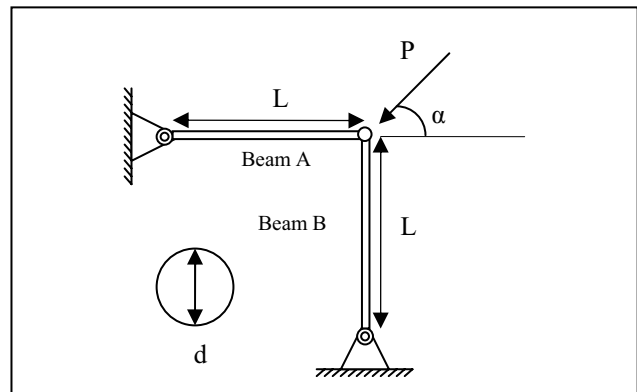


FIG. 7 Two member system with angled loading

The structure was initially designed such that the angle, α , at which the load, P is applied, would be 45° from the horizontal. Given that the two beams are hinged to each other and pin-jointed at the edges, only axial compression should occur. The applied load, P is also the critical load as defined by Euler as shown below:

$$(9) \quad P_{cr} = k \frac{\pi^2 EI}{L^2}$$

The moment of inertia, I for the beam is:

$$(10) \quad I = \frac{\pi d^4}{64}$$

In this case, $k = 1$. If the angle, α is greater than 45 degrees, then it is expected that Beam A should not fail under buckling. TAB. 3 below shows the stochastic boundary of this analysis. A standard deviation of 1% has been used to show that even though small tolerances are used, failure can still occur.

TABLE 3

Input Variable	Mean	Defined Range
Load, P (N)	299 752.5	Constant
Angle, α (deg)	50	46.25 - 53.75
Length, L (mm)	1 000	970 - 1 030
Young's Modulus, E (MPa)	70 000	67900 - 72100
Diameter, d (mm)	50	46.25 - 53.75

A sample size of 100 was used for the stochastic analysis. FIG. 8 and FIG. 9 show the relationship between the inputs and the critical load while FIG. 10 is a metamodel describing the occurrence of failure due to buckling, with respect to the angle of the applied force.

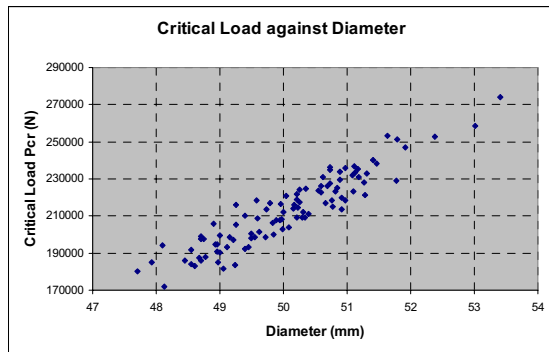


FIG. 8 Metamodel of critical load against diameter

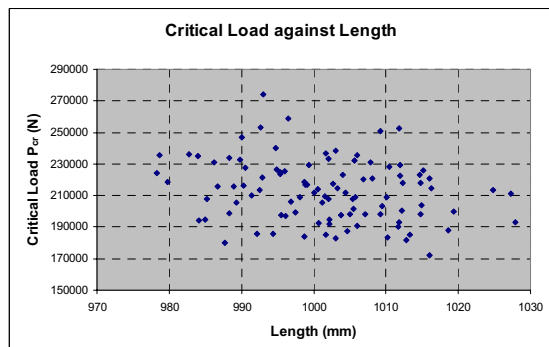


FIG. 9 Metamodel of critical load against length

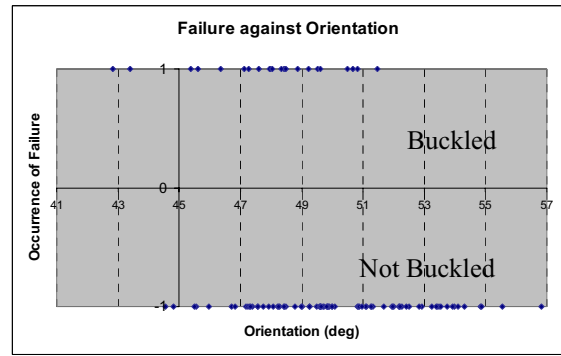


FIG. 10 Metamodel of failure against orientation

From the figure above, it can be seen that failure occurs more frequently than previously thought. In a single analysis with deterministic variables, this may not have been the case. Hence there is a need to use stochastic in order to show the range of possibilities that might have otherwise been ignored. TAB. 4 shows the influence that each variable has over the critical load.

TABLE 4

Relationship	Spearman Correlation
Critical Load and Young's Modulus	0.223
Critical Load and Diameter	0.924
Critical Load and Length	-0.189

3. SFEA FOR CURVED STIFFENED PANELS

A stochastic analysis was applied to a fuselage-representative multi-stiffener panel design from the COCOMAT project. Boundary conditions and material properties similar to those prescribed within COCOMAT were used as the benchmark deterministic analysis. The net axial compression applied was 4 mm for all analyses. Both ends of the panel are fixed in a manner similar to the potting in the physical model. FIG. 11^[11] below shows preparation of a curved panel for testing where potting has been added. The analyses were solved using MSC.Marc. Nominal dimensions and material data are given below in TAB. 5.

TABLE 5

Panel Length (mm)	780
Panel Free Length (mm)	660
Panel Radius (mm)	1 000
Stiffener Pitch (mm)	129
Number of Stiffeners	5
Panel Arc Length (mm)	560
Stiffener Width (mm)	32
Stiffener Height (mm)	14
Material System	Hexcel IM7/8553
Skin Lay-up	[90, ± 45 , 0] _s
Stiffener Web Lay-up	[(45,-45) ₃ , 0] ₆ _s
Stiffener Flange Lay-up	[0 ₆ , (45,-45) ₃]

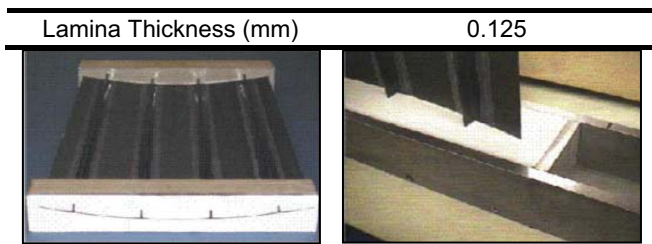


FIG. 11 Preparation of Test Panel [11]

3.1 Stochastic Parameters

A multi-variant approach as shown in the previous section was taken to conduct the stochastic analysis. Each run consisted of all the material, laminate and boundary condition input variables being varied within the ranges defined in TAB. 6 and 7. Each run consisted of 100 properties being varied for each stiffened panel. There were 20 runs in total.

3.1.1 Material and Lamina Properties

Gaussian normal inputs were chosen for the input variables. The variation chosen for the ply orientations was 2.5%. This corresponds to the ply orientations and thicknesses having a first standard deviation of 1.125 degrees. The remainder input variables such as material properties and lamina thickness had a variation of 5%. Each individual stiffener had stochastic orientations and thicknesses. The following variables were included in the SFEA:

- 1) Lamina Thickness
- 2) Lamina Orientation
- 3) Young's Modulus
- 4) Shear Modulus
- 5) Poisson's Ratio

TAB. 6 below shows the deterministic input values and the corresponding stochastic variation used. The values in the defined range are from -3 to +3 standard deviations from the mean.

TABLE 6

Input Variable	Mean	Defined Range	
Young's Modulus E_{11} (MPa)	147 000	124 950	- 169 050
Young's Modulus E_{22} (MPa)	11 800	10 030	- 13 570
Poisson's Ratio ν_{12}	0.34	0.289	- 0.391
Shear Modulus G_{12} (MPa)	6 000	5 100	- 6 900
Shear Modulus G_{23} (MPa)	4 000	3 400	- 4 600
Shear Modulus G_{13} (MPa)	6 000	5 100	- 6 900
0° Lamina (deg)	0	-3.375	- 3.375
45° Lamina (deg)	45	41.625	- 48.375
-45° Lamina (deg)	-45	-41.625	- 48.375
90° Lamina (deg)	90	86.625	- 93.375

Ply Thickness (mm)	0.125	0.106	-	0.144
--------------------	-------	-------	---	-------

3.1.2 Boundary Conditions

The treatment of the boundary conditions was meant to reflect the possible loading and potting conditions. The boundary conditions simulating the potting and fixed edge of the panel were kept as per the original finite element model. A new node was created at the centre of curvature and an RBE2 MPC was created to link all the nodes on the shortened edge to the new node. This was done in order to introduce linear loading onto the panel. FIG. 12 below illustrates the created node and MPC.

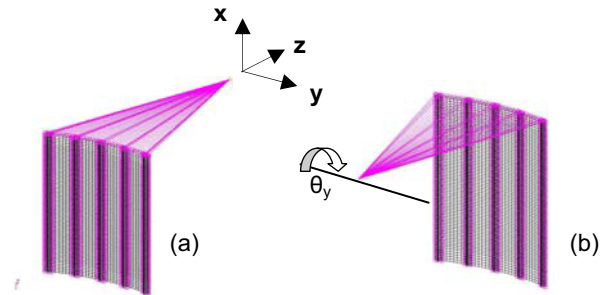


FIG. 12 Illustration of created Node and MPC

Variation for the boundary condition was introduced via the application of translation and rotation displacements onto the new node. The rotations about the y-axis have been included such that the tip of the stiffener blade has an axial displacement range of ± 0.1 mm when compared to the skin. The resulting applied displacements as shown below in TAB. 7 take into consideration the axial displacement experienced by the panel when rotational displacement is applied onto the MPC such that the resultant displacement was 4 mm about the neutral axis. An example of the stochastic boundary condition for the displacement can be seen below. TAB. 7 shows the defined range for the variables. The applied displacement is dependent on the applied rotation; all axial compression is 4 mm about the neutral axis.

TABLE 7

Input Variable	Mean	Defined Range	
Applied Displacement (mm)	4	<i>dependent on rotation</i>	
Applied Rotation, θ_y (deg)	0	-1.225	- 1.225

4. RESULTS AND DISCUSSION

Under compression, the stiffened panels developed a number of buckling shapes, including skin buckling between the stiffener, or local buckling, and buckling of the stiffeners themselves, or global buckling. Following global buckling of the stiffeners, in the postbuckling region, the panels developed a number of different postbuckling mode shapes involving global buckles in two or three buckles of the stiffener bays. For all analyses the postbuckling mode shape seen at the end of the 4 mm compression illustrated the symmetric or asymmetric behaviour of the panel, and these were used for comparison of panels. From the

analyses, there were two deep postbuckling modes obtained through stochastic lamina and material properties which are given in FIG. 13.

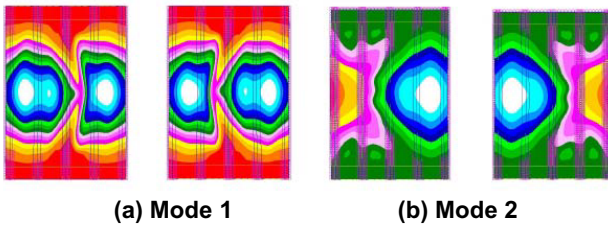


FIG. 13 Deep postbuckling mode shapes seen in stochastic analysis

The experimental results were presented previously in FIG. 1, where it was illustrated that an asymmetric postbuckling mode developed that was not captured by the deterministic analysis. Consequently, the stochastic analysis was focused on determining the influence of the panel parameters on the mode shape.

From the SFEA it was seen that the buckling mode shape from varying only the material and lamina properties did not cause asymmetrical buckling modes. Variation in laminate stiffness ultimately affects the magnitude of the out of plane displacement as well as the postbuckling failure sequence. However, it was found that there was a strong correlation between the application of an angular displacement and the final postbuckling mode shape. A positive angular displacement about the y -axis in FIG. 12 parallel to the global y -axis caused the panel to assume an asymmetrical postbuckling mode. The agreement between the asymmetric buckling patterns of the experimental and SFEA panel with the angular rotation boundary condition is illustrated in FIG. 14.

The inclusion of other noise variables such as material and lamina properties serves to vary the magnitude of the out of plane displacement due to the changes in laminate stiffness as well as the failure progression once the postbuckling region has been reached. This difference can be observed in FIG. 14. Hence it is plausible that in future COCOMAT experiments, variation in the results should be expected as imperfections will be introduced into the panels during manufacture and testing.

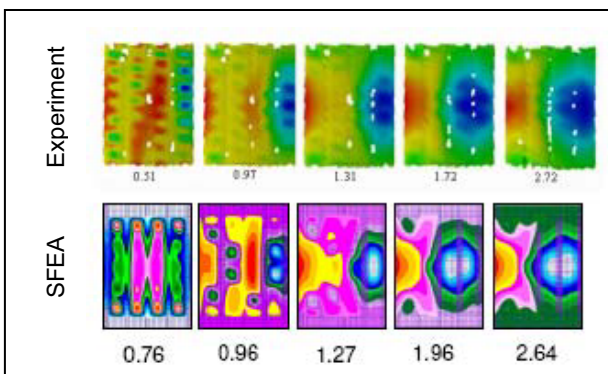


FIG. 14 Comparison of experimental and SFEA results

4.1 Bifurcation in Postbuckling Mode shape

From the SFEA, it is evident that a major cause of the asymmetry can be attributed to a greater displacement being applied to the stiffeners and the inner surface of the skin laminate due to the extra rotational displacement. A metamodel of 20 samples is shown below in FIG. 15 where the postbuckling mode shape has been plotted against the applied angular rotation. Note the bifurcation region that exists in the metamodel. Within this region, it is possible for the panel to have 2 postbuckling mode shapes. A Spearman Correlation between the mode shape and orientation angle was found, and the correlation strength was 0.72 which indicates a very strong relationship. Another notable contribution of the difference in mode shapes is from the coupling stiffness B_{11} of the skin. The correlation between B_{11} and the mode shape is 0.304. TAB. 8 below shows the correlation between the input variables and mode shape.

TABLE 8

Relationship of Variable against Mode		Spearman Correlation
Skin	A_{11}	-0.018
	B_{11}	0.304
	D_{11}	-0.110
Flange	A_{11}	-0.193
	B_{11}	-0.135
	D_{11}	-0.122
Web	A_{11}	0.012
	B_{11}	0.032
	D_{11}	-0.055
Material Properties	E_{11}	0.030
	E_{22}	-0.110
	ν	0.173
	G_{12}	-0.048
	G_{23}	-0.038
	G_{31}	-0.293
	Orientation	0.720

Once all the experiments in COCOMAT are completed, there will inevitably be a degree of scatter in the results. This is expected to correlate with the bifurcation seen in FIG. 15 where symmetrical and asymmetrical postbuckling mode shapes are possible. This will in turn lead to differing load-shortening curves being obtained, which will affect the use of the results for validation of any developed numerical models. Recommendations for limiting the experimental variation in buckling shape are discussed in the following section.

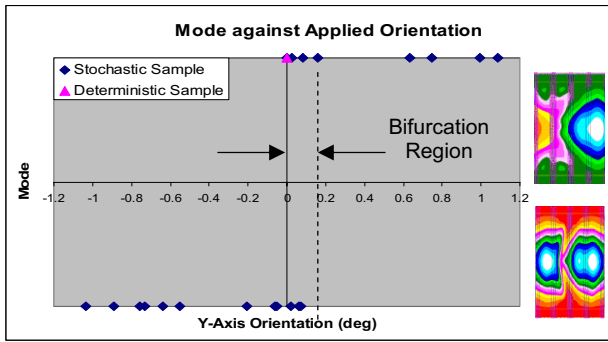


FIG. 15 Metamodel of mode shape against applied rotation

A pure compression scenario that has been modelled using the benchmark deterministic model will always produce a symmetrical postbuckling mode shape. When a finite element model utilising nominal design variables is subjected to a compression translation and rotation, it also results in an asymmetrical postbuckling mode shape. This shows the sensitivity or lack of robustness in the stiffened panel, and it can be seen in the figure that this sensitivity increases once imperfection is included in the material and laminate properties. The difference in the global buckling sequence can be seen in the load shortening curve below in FIG. 16. It can be observed that there is a significant difference in the load carrying capability of the panel depending on the postbuckling mode shape.

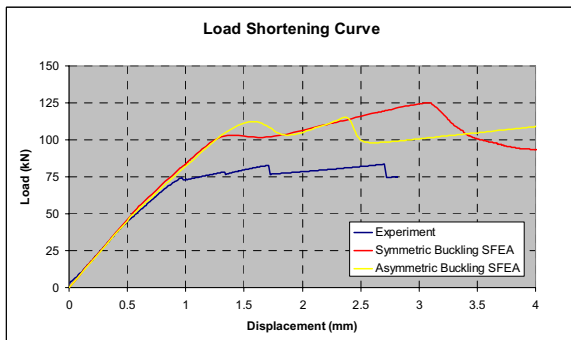


FIG. 16 Applied load versus compression for the experiment and FE panels, showing symmetric and asymmetric FE results

4.2 Coupling of Bending and Compression

As the curved panel is compressed in the longitudinal axis, Poisson's effect causes the panel to expand transversely. This expansion can lead to out of plane displacement as the constraint imposed by the end conditions resists an increase in the transverse dimension of the plate. This behaviour is similar to the anticlastic bending of thin plates^[15]. A moment has been introduced onto the edge of the panel via the rotational displacement. FIG. 17 below illustrates this behaviour at the mid-longitudinal plane of the panel. The outer surface of the panel has a lower compressive force compared to the inner surface. This difference in force induces a moment about the mid-plane of the panel. As the moment increases, the panel deforms into the shape shown to fulfil compatibility and continuity as the inner surface has a circumference greater than the

outer surface.

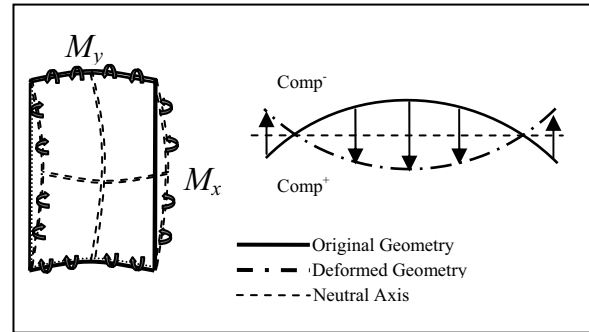


FIG. 17 Anticlastic bending of curved panel

In the case of the laminates in COCOMAT that are anisotropic, the various skin laminae will have different transverse expansions due to the different thicknesses and orientations. The result of this complex interaction between lamina can be seen in FIG. 14 where the panels adopt two half sine waves along the transverse axis. It can be seen that the local buckles close to the middle stiffener combine into a larger global buckle that is of opposite out of plane displacement compared to those at the longitudinal edges. As axial compression is applied, the middle stiffener rotates and the moment created promotes the asymmetry of the panel displacement. The rotational displacement of the middle stiffener at different axial compression levels is given in FIG. 18.

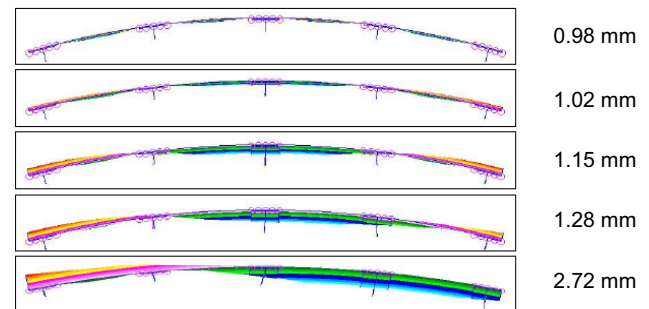


FIG. 18 Rotational displacement of middle stiffener

The benchmark FE analyses had buckled regions along the longitudinal edge and an out of plane displacement greater than that of the middle stiffener. Hence as more axial displacement was applied, the buckles along the longitudinal edges increased in magnitude, causing the buckle at the middle stiffener to disappear.

Referring to the experimental results in FIG. 14, it was observed that the local buckling lead to the formation of two half sine waves across the transverse axis of the panel. This panel was manufactured on a voluntary basis in the COCOMAT project, and the strict manufacturing procedure for the standard COCOMAT panels was not applied. This meant that there was a larger scope for variation in manufacturing and in application of the load. This matches the input variables for the stochastic finite element run where the variables also had a larger deviation from the nominal mean.

The failure scenarios as described above where more compression is applied onto the inner surface can be translated to the edges of the potting not being absolutely

parallel with the contact surfaces on the axial testing machine. It is highly probable that this occurred during the manufacturing phase where the potting was added onto the composite panel. After the potting had set, the edges were machined to ensure uniform flatness. No checks were made to ensure that both edges were parallel after the machining. Also, if the stiffener has defects that cause premature buckling, a similar situation will occur where the blade will buckle into a half sine wave, causing the flange to introduce asymmetrical stress into the skin.

At the material level, composites exhibit fibre, matrix or fibre-matrix interface failures. Material degradation and disbonding has not been introduced in the stochastic analyses described in this paper. In order for more accurate matching of numerical and physical results, this should be done in the future.

4.3 Designing for One Postbuckling Mode

It is always desirable to design for experiments and structures to fail in one mode as opposed to multiple modes. Likewise for COCOMAT, it would be helpful in the interpretation of experimental data, if all the panels are designed to fail in one mode. Two methods have been identified in order to produce a single postbuckling mode. The first involves the redesign of the experiment while the second requires a redesign of the composite panel itself.

Redesigning the experiment might have a cost penalty, but it would be a logical step to take if reality is to be incorporated. The experimental rig should include a rotational component onto the top and bottom edges of the test pieces. The induced rotation should be positive as seen in FIG. 15 so that the bifurcation in postbuckling behaviour does not occur. This is similar to the compression of aircraft fuselages where compression is about the centroid of the fuselage body and the outer skin is subject to greater stresses compared to the inner skin.

The second option of redesigning the panel means that more longitudinal stiffness has to be provided to the inner skin. Finite element analyses with an increase in blade stiffness have given symmetrical postbuckling mode shapes. The stiffer blade increases the buckling load of the panel and also allows some stress to be transferred from the inner skin onto the blade.

5. CONCLUSION

Finite element analyses involving a stiffened curved composite panel employing stochastic material properties and boundary conditions have been conducted. Since the postbuckling mode shapes affect the numerical results, it is important that the physical experiments be captured and matched in the FE environment. The purpose of introducing stochastic input variables was to show various buckling modes do occur and that these variations can be expected when the physical panels are tested.

The prediction of structural failure is always difficult as failure is never caused by a single variable; it is always a case of a combination of variables. Introducing stochastic variables enables the FE simulations to take on multiple cases for loading, geometrical and material properties. This enables engineers to move from curve-fitting towards a scenario where possibilities lie within a cloud or region, thereby simulating the stochastic nature of reality.

It is a recommendation of the authors that for future projects, stochastic analyses can be conducted during benchmarking and during design of the specimen. The rationale behind this is so that any bifurcation behaviour in the postbuckling region that might otherwise occur can be avoided during design or understood as it appears in the results.

The success of this analysis depends on the pool of variables considered. In practise the selection of input variables for an analysis really depends on experience. A literature survey was conducted on the buckling of panels as seen in the introduction. This led to the conclusion that the dominant variables controlling the postbuckling modes and loads were the boundary conditions in addition to the material and geometrical properties. This was the source of insight for including the applied rotation as well as variation in the material and geometry.

6. ACKNOWLEDGEMENTS

The authors would like to acknowledge the financial support of the Cooperative Research Centre for Advanced Composite Structures (CRC-ACS) Ltd. This research has also been done using experimental data obtained from DLR Institute for Composite Structures and Adaptive Systems, Braunschweig, Germany.

7. REFERENCES

- [1] Degenhardt, R., Rolfes, R., Zimmermann, R., Rohwer, K., COCOMAT - Improved Material Exploitation of Composite Airframe Structures by Accurate Simulation of Postbuckling and Collapse, *Composite Structures* 73 (2006) 175 -178
- [2] Orifici, A. C., Thomson, R. S., Degenhardt, R., Kling, A., Rohwer, K., Bayandor, J., Degradation Investigation in a Postbuckling Composite Stiffened Panel', *Composite Structures* 2007, doi: 10.1016/j.compstruct.2007.01.012.
- [3] Chryssanthopoulos, M. K., Poggi, C., Stochastic Imperfection Modelling in Shell Stiffened Studies, *Thin-Walled Structures* 23 (1995) 179-200
- [4] Orifici, A. C., Thomson, R. S., Gunnion, A. J., Degenhardt, R., Abramovich, H., Bayandor, J., Benchmark Finite Element Simulations of Postbuckling Stiffened Composite Panels, *11th Australian International Aerospace Congress Melbourne Australia*, 13-17 Mar 2005
- [5] Raj, B. N., Iyengar, N. G. R., Yadav, D., Response of Composite Plates with Random Material Properties using FEM and Monte Carlo Simulation, *Advanced Composite Materials* 7(3) (1998) 219-237
- [6] Singh, B. N., Iyengar, N. G. R., Yadav, D., Stability of Curved Composite Panels with Random Material Properties, *Journal of Aerospace Engineering* 15(2) (2002) 46-54
- [7] Yadav, D., Verma, N., Buckling of Composite Circular Cylindrical Shells with Random Material Properties, *Journal of Composite Structures* 37(3-4) (1997) 385-391
- [8] Noor, A. K., Starnes, J. H., Peters, J. M., Curved Sandwich Panels Subject to Temperature Gradient and Mechanical Loads, *Journal of Aerospace Engineering*, 10(4) (1997) 143-161

- [9] Shiao, M. C., Chamis, C. C.,
Probabilistic Evaluation of Fuselage-type Composite
Structures, *Probabilistic Engineering Mechanics* 14
(1999) 179-187
- [10] Chamis, C. C.,
Probabilistic Simulation of Multi-scale Composite
Behavior, *Theoretical and Applied Fracture
Mechanics* 41 (2004) 51-61
- [11] Zimmermann, R., Klein, H., Kling, A.,
Buckling and Postbuckling of Stringer Stiffened Fibre
Composite Curved Panels - Tests and Computations,
Composite Structures 73 (2006) 150-161
- [12] Short, G. J., Guild, F. J., Pavier, M. J.,
Delaminations in Flat and Curved Composite
Laminates Subjected to Compressive Loads,
Composite Structures 58 (2002) 249-258
- [13] Marczyk, J.,
Does Optimal Mean Best?, *MSC Software Virtual
Product Development Conference EMEA* (2004)
- [14] Spearman, C.,
Demonstration of Formulae for True Measurement of
Correlation, *The American Journal of Psychology*
18(2) (1907), 161-169
- [15] Timoshenko, S. P., Woinowsky-Krieger, S.,
Theory of Plates and Shells, 2nd Ed., McGraw-Hill
Book Company, New York, (1959)